An Update to Probable Maximum Precipitation Accounting for More Than Moisture Availability Alone: A Case Study of Nepal.

Supplementary Material

[Asphota Wasti[1*], Katherine Schlef[2], Bill Kappel[3], Saiful Haque Rahat[4], Gaurav Atreya[1], Amy Townsend-Small[5], Patrick Ray[1]]

[1] Department of Chemical and Environmental Engineering, College of Engineering and Applied Science, University of Cincinnati

[2] Department of Civil and Environmental Engineering, College of Engineering, Western New England University

[3] Chief Meteorologist, Applied Weather Associates

[4] Geosyntec Consultants, 920 SW 6th Ave Suite, 600, Portland, OR 97204, United States of America

[5] School of Environment and Sustainability Studies, College of Arts and Sciences, University of Cincinnati

*Corresponding author: Asphota Wasti, wastiaa@mail.uc.edu

Keywords: Probable Maximum Precipitation, Maximization Approach, Precipitable Water, Convective Available Potential Energy, Vertical Wind Velocity

1. Distribution of Extreme Precipitation in Nepal

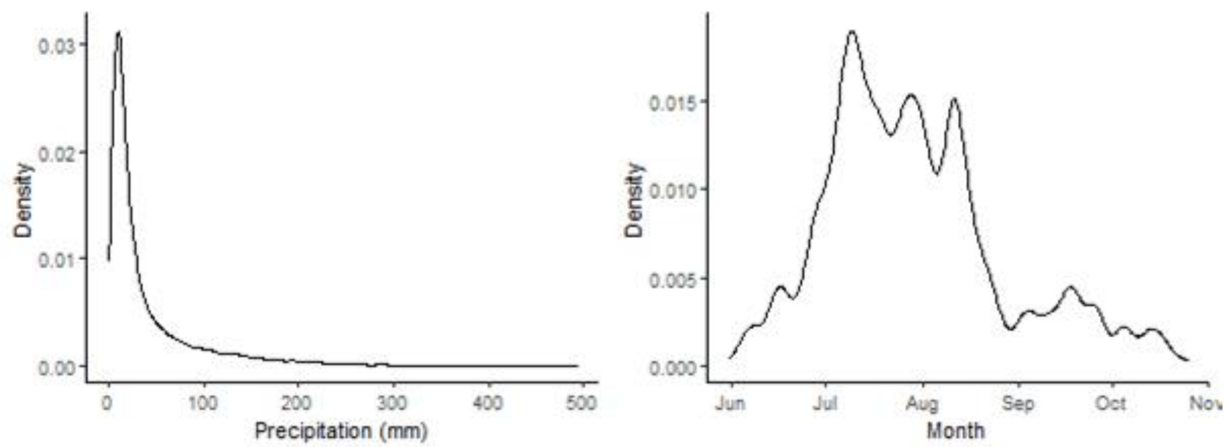

S 1 Distribution of the top-50 maximum 3-day precipitation in the area of study. The figure shows that the 3-day extreme precipitation is concentrated between June – August.

2. Correlation between Precipitable Water Vapor and Relative Humidity

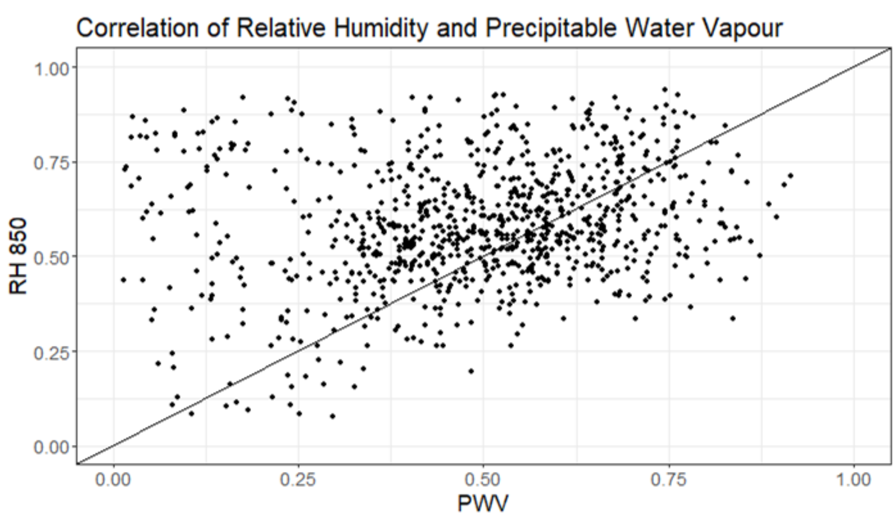

S 2 Correlation between *PW* and *RH*. The figure shows that Relative Humidity is strongly related to Precipitable Water and thus is a redundant atmospheric variable in the analysis.

3. Additional Analysis in the Screening Process : Sensitivity to Pressure Level

The spatial distribution of the proportion of the atmospheric variables as the atmospheric pressure levels are changed is presented in S 3. In the figure, the Vertical velocity (V_{velo}) is plotted at 700 hPa and 750 hPa; and the northward component of wind velocity (V_{wind}) is plotted at 750 hPa for illustration. In the study, the proportions of atmospheric variables at the atmospheric pressure of 850 hPa are analyzed. These figures illustrate that the spatial distribution of the weights of the variables is preserved and re-evaluated for a different pressure level. Refer to Figure 3 in the main paper to see the illustration for the 850 hPa.

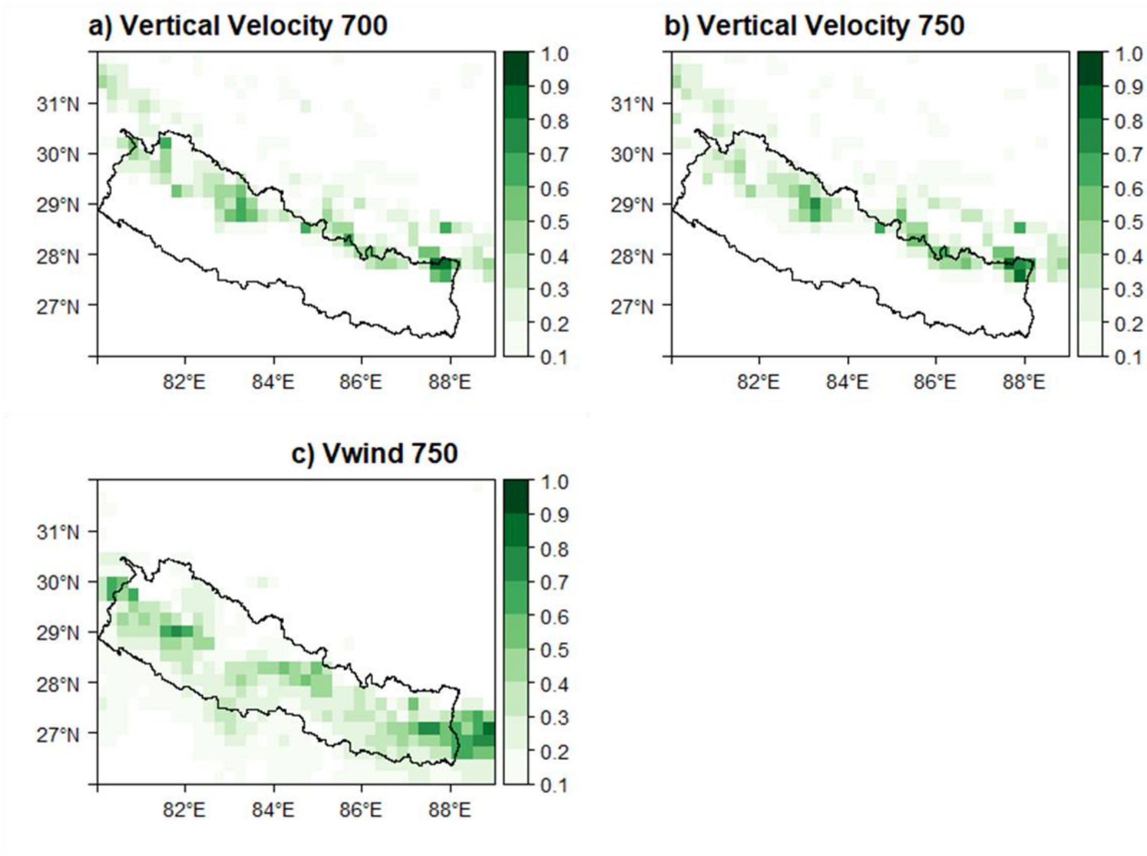

S 3 Some examples of atmospheric variables at different pressure levels than the ones used in the analysis. Here the dominance for V_{velo} is plotted at 700 hPa and 750 hPa and the dominance for V_{wind} is plotted at 750 hPa for illustration. In the study, these variables at 850 hPa were analyzed. Refer to Figure 3 in the main paper.

4. Additional Analysis in the Screening Process: Storm Duration

The spatial distribution of the proportion of the atmospheric variables with change in storm duration was studied. S 4 illustrates the distribution of if 1-day maximum precipitation were to be analyzed and S 5 illustrates the distribution of 2-day maximum precipitation were to be analyzed. These figures illustrate that the spatial distribution of the weights of the variables is preserved when the duration of the storm is changed. Refer to Figure 3 in the main paper to see the illustration for the 3-day maximum precipitation.

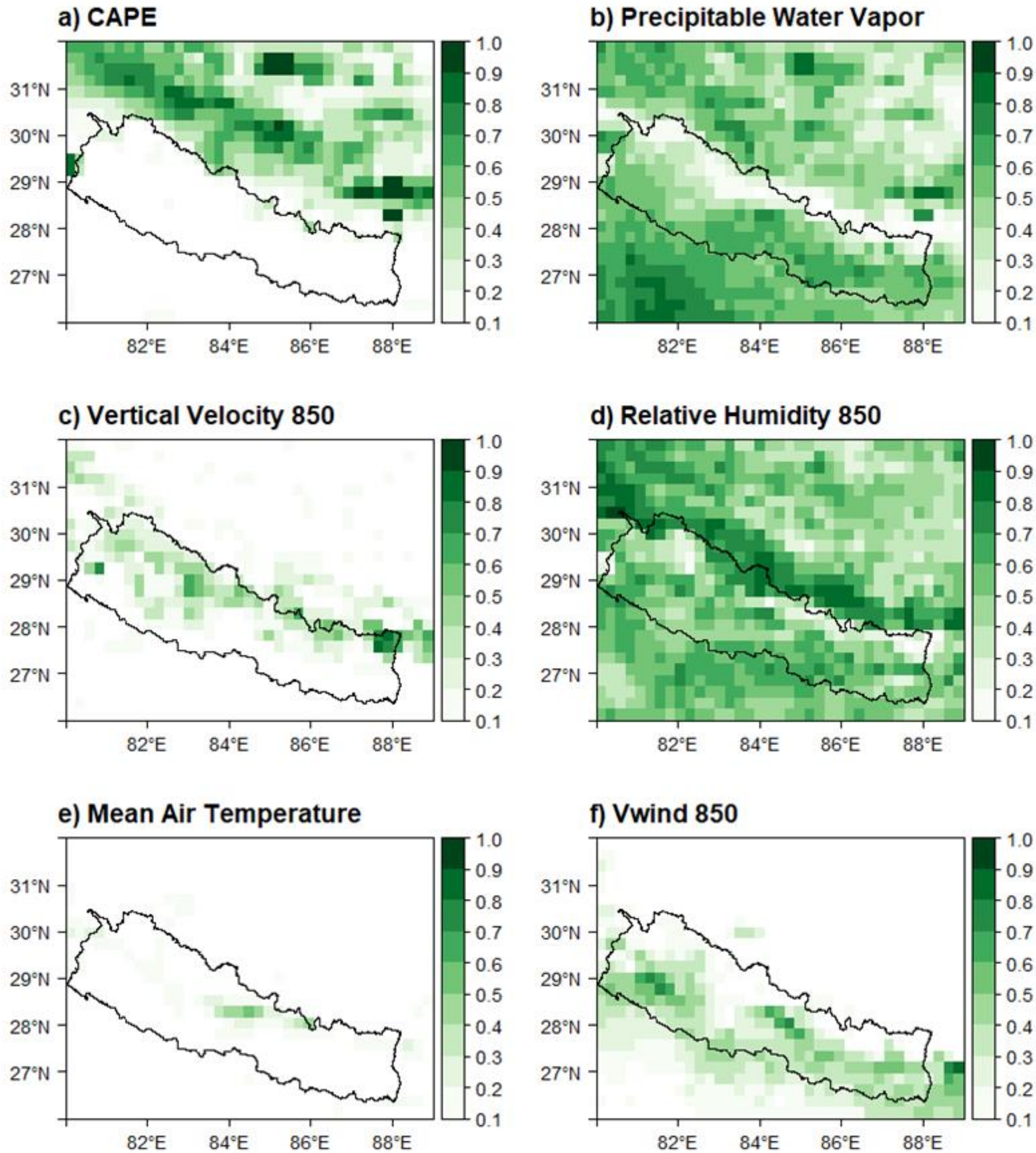

S 4 Illustration of the spatial distribution of the proportion of the atmospheric variables in the upper 90th percentile for a 1-day storm.

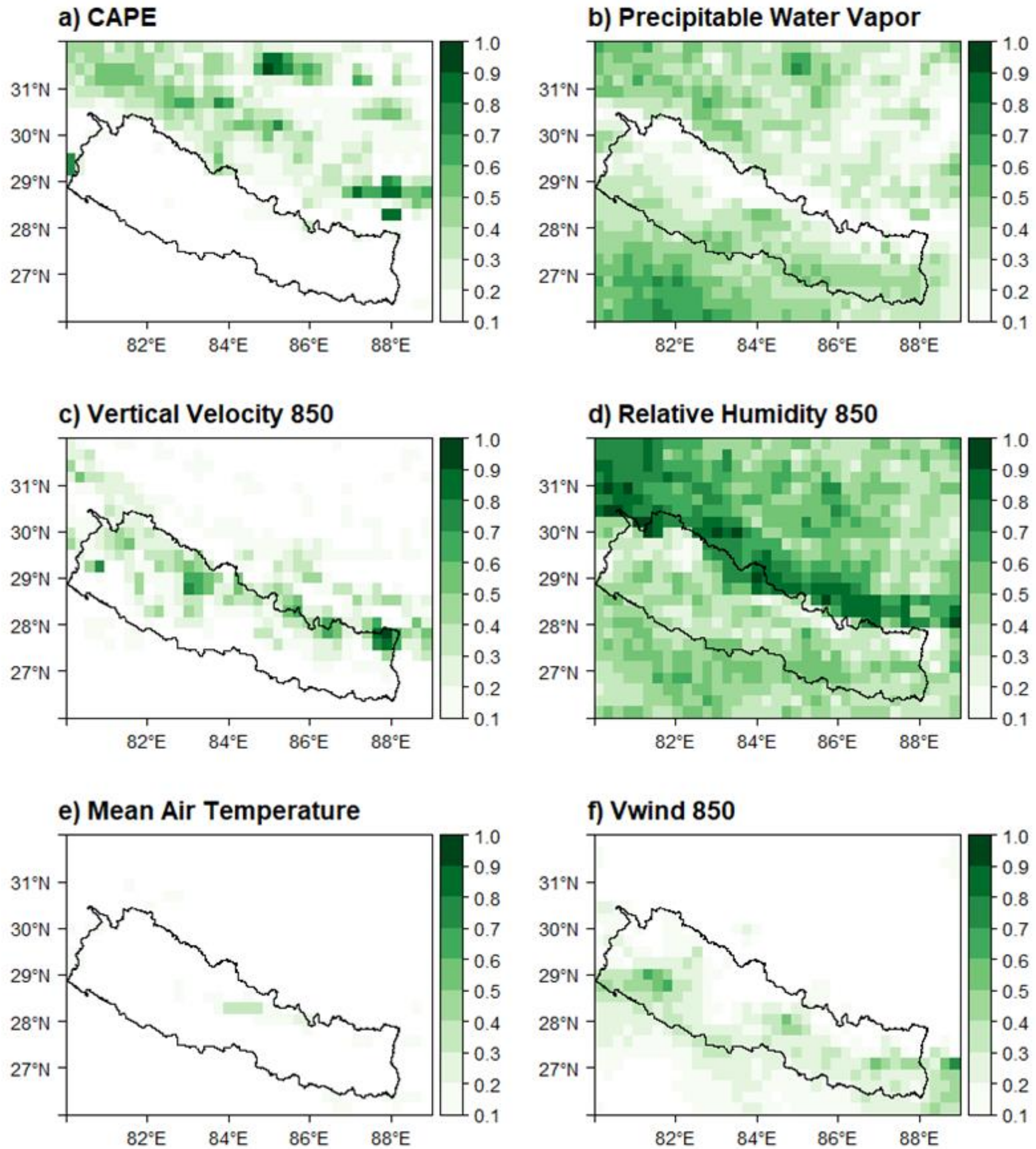

S 5 Illustration of the spatial distribution of the proportion of the atmospheric variables in the upper 90th percentile for a 2-day storm.

5. Sensitivity Analysis of the Screening Process: Choice of θ and N

The values and the spatial distribution of the weights of the dominant atmospheric variables are affected by the choice of the two parameters (θ, and N).

We tested the sensitivity of our results to the choice of the number of historical events analyzed (N) by varying the number of events between 25 and 100. The most influential atmospheric variable with the maximum weight, max (w_i), is illustrated as N is set to a) 25, b) 50, and c) 100 respectively in S 6. The sensitivity analysis indicates that the spatial distribution of the dominant atmospheric variable is preserved even when the thresholds are varied. If N is set closer to 100, the criteria become overly generalized, and insights from the atmospheric variable are lost amongst other data noise. If we reduce the sample size nearer to 25, the criterion becomes overly-restrictive and does not capture the natural variability of the atmospheric variables. For our study, the choice of 50 events **($\boldsymbol{N = 50}$)** was found to balance precision and inclusivity (emphasized with dotted lines in S 6).

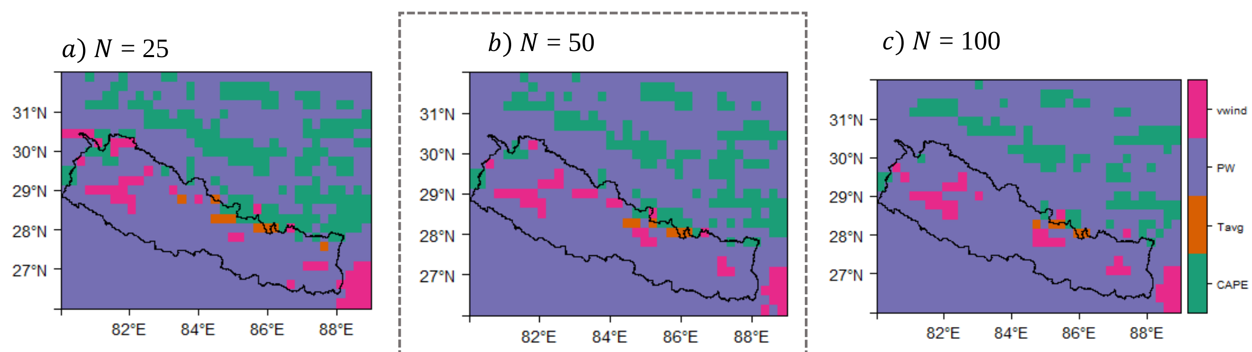

S 6 Sensitivity of the most dominant atmospheric variable driving the 3-day extreme precipitation to the choice of number of events, $\boldsymbol{N}$. The variables $\boldsymbol{CAPE}$, $\boldsymbol{PW}$, $\boldsymbol{V_{wind}}$, and $\boldsymbol{T_{avg}}$ are represented by the colors green, purple, pink, and orange, respectively.

Figure 1

Similarly, we tested the sensitivity of the results to the choice of the threshold placed on the CDF curve (θ) by varying the threshold between the 85th to 95th percentile. The most influential atmospheric variable with the maximum weight, max (w_i), is illustrated as the threshold θ is set to a) 0.85, b) 0.9, and c) 0.95, respectively, in S 7. The sensitivity analysis indicates that the spatial distribution of the dominant atmospheric variable is preserved even when the thresholds are varied. The choice of the 95th percentile is overly-restrictive, and the 85th percentile is overly-general. For our study, the choice of the 90th percentile ($\boldsymbol{\theta = 0.90}$) was found to balance precision and inclusivity (emphasized with dotted lines in S 7).

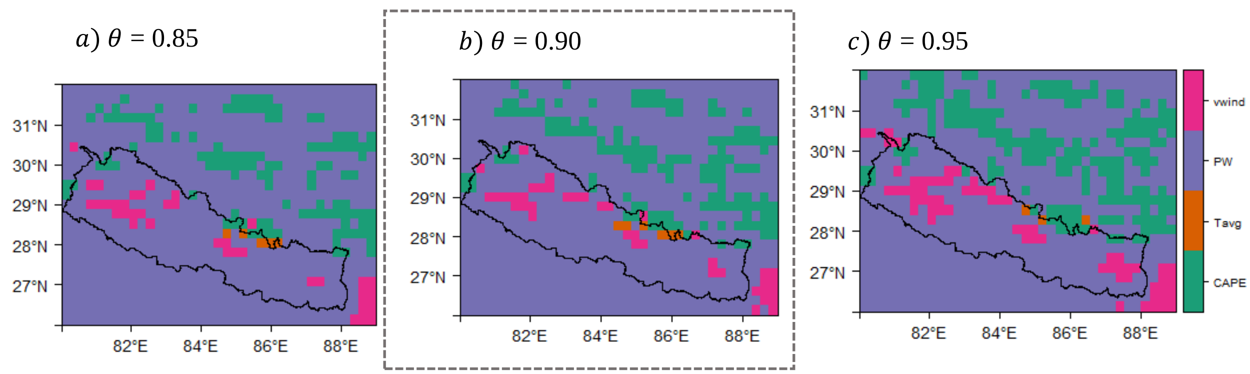

S 7 Sensitivity of the most dominant atmospheric variable driving the 3-day extreme precipitation to the choice of threshold $\boldsymbol{\theta}$. The variables $\boldsymbol{CAPE}$, $\boldsymbol{PW}$, $\boldsymbol{V_{wind}}$, and $\boldsymbol{T_{avg}}$ are represented by the colors green, purple, pink, and orange, respectively.

6. Additional Analysis to Support the Screening Process

The weight of an atmospheric variable (x-axis) is plotted against the correlation between the atmospheric variable and precipitation (y-axis) in S 8. It is observed that the correlation increases with an increase in weight for $CAPE$, and V_{wind}. PW, demonstrating a monotonic relationship between extreme precipitation and the weights of the variables. T_{avg}, shows weak correlation with extreme precipitation, and is included in the analysis for illustration purposes.

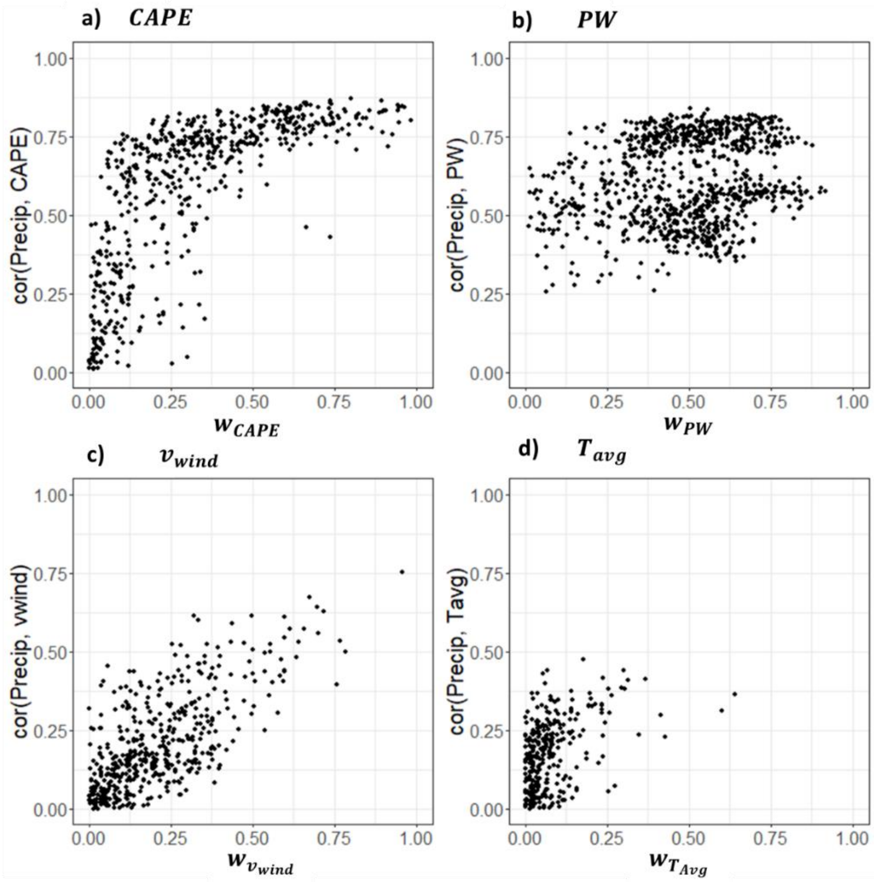

S 8 Correlation of the precipitation with an atmospheric variable is plotted against the weight of the atmospheric variable for a) $CAPE$, b) PW, c) v_{wind}, and d) T_{avg}.

7. Interpretation of the Patterns of Drivers of Extreme Precipitation

In this section, we analyze the spatial patterns of the weights of the dominant atmospheric variables. The weights of the variables are plotted against latitude and elevation to identify spatial patterns (Figure 2).

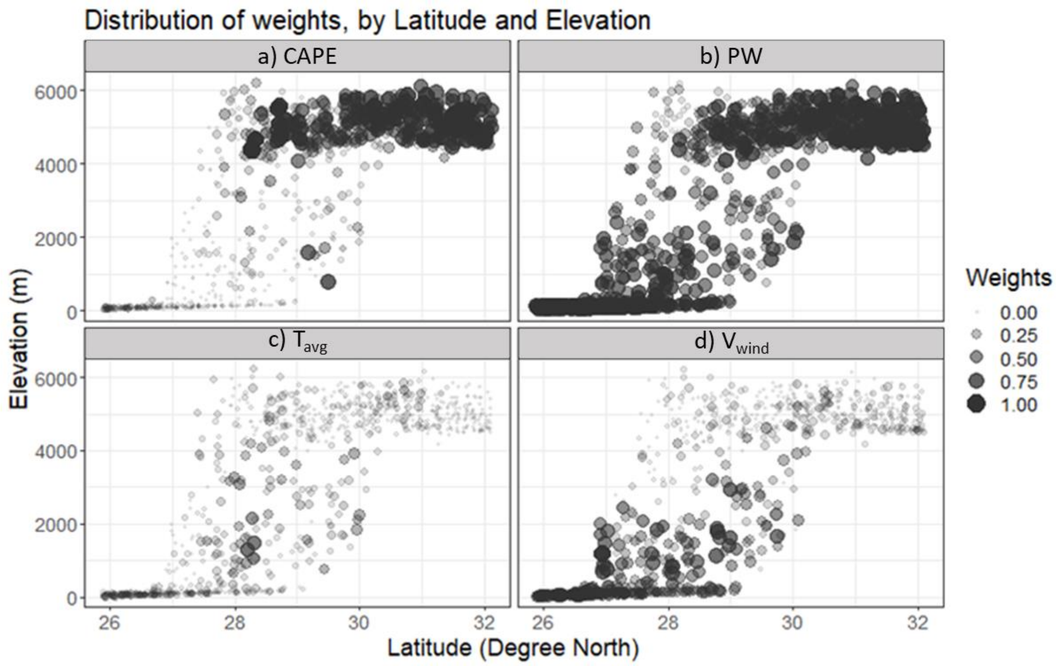

Figure 2 Distribution of weights of dominant atmospheric variables by latitude and elevation.

CAPE: $CAPE$ indicates the (in)stability of the atmosphere. Higher $CAPE$ represents a high potential for the development of convection and heavy rainfall, often accompanied by a thunderstorm. We observe that the w_{CAPE} is high in elevation between 4000 m and 6000 m. Topographically, this region is the area on the northern leeward side of the Himalayas. This is likely because there is a lack of sustained low-level moisture access in this region. Therefore, moisture at the mid and upper levels of the atmosphere results in precipitation. However, to convert moisture in the mid and upper levels of the atmosphere to precipitation on the ground, significant vertical motions through a large depth of the atmosphere i.e., higher $CAPE$ is needed.

PW: PW is the most prominent driver of extreme precipitation. We observe that the w_{PW} is generally high everywhere except in the elevation range of 2000 m – 4000 m. Topographically this elevation range represents the region between the foothills and the rising windward side of the Himalayas. Most likely, PW is not the dominant factor for extreme precipitation in this elevation range on the windward side of the Himalayas due to the higher influence of the orographic effect. In the leeward side of the Himalayas, both $CAPE$ and PW are dominant drivers of extreme precipitation.

T_{avg}: We observe the values of $w_{T_{avg}}$ is uniform and below 0.25, with a few local exceptions. The low values of $w_{T_{avg}}$ suggest that average temperature by itself has the least influence on extreme precipitation. However, an increase (or decrease) in temperature has the potential to affect other atmospheric variables, which in turn may influence extreme precipitation.

V_{wind}: We observe that the values of $w_{V_{wind}}$ are observed to be high below 2000 m between 26^0 N and 30^0 N. Topographically, this region of high concentration of large $w_{V_{wind}}$ corresponds to the major valleys in the mid-hills of Nepal. During the Indian summer monsoon, moisture-laden winds flow northward toward the Himalayas. Wind flow in narrowing valleys may induce horizontal convergence and resultant vertical lift of moisture initiating or increasing precipitation [17]. These pockets of high $w_{V_{wind}}$ may be an indicator of such phenomena.

8. Correlation between the Terms in the Combined Maximization

The correlation between the terms when calculating the weighted average for combined maximization ratio in S 9. The terms shown in S 9 are not correlated, except for the products of weights and ratios of PW and $CAPE$ (highlighted in red rectangle). Within the highlighted red rectangle, the points along the diagonal show a strong (1:1) relation between $w_{CAPE}r_{CAPE}$ and $w_{PW}r_{PW}$, which represents the regions where both the variables have a similar overall influence on extreme precipitation. In this study, this correlation is not accounted for when calculating the weighted average.

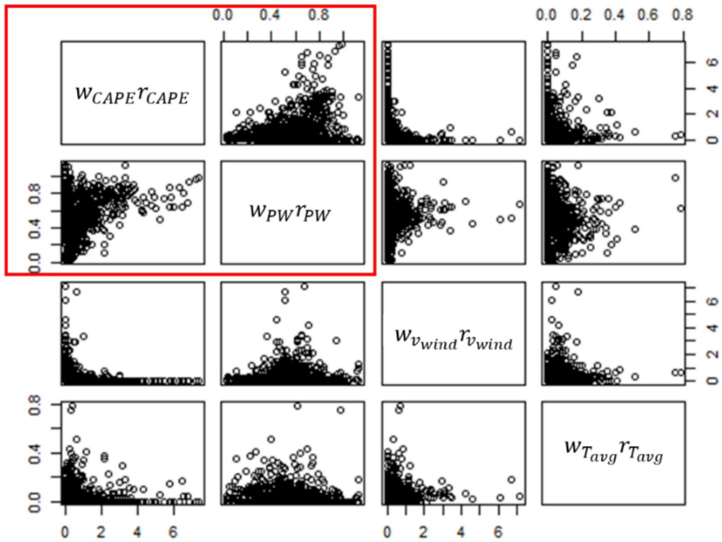

S 9 A correlation plot for the products of weights and ratios of atmospheric variables.